Chapter 4

Luminescence properties of Tb, Er doped GaN and comparative studies with Eu doped GaN.

Tb doped GaN and Er doped GaN were studied aimed for the material of green emission. Er doped GaN has another way of practical application on using infra-red emission. In this chapter, single crystalline growth of Tb doped GaN and Er doped GaN were carried out and material properties were reviewed. Comparative studies between Eu doped GaN discussed as well.

4.1 The growth and characterization of Tb, Er doped GaN.

The RHEED patterns of Tb doped GaN and Er doped GaN after 2 hour growths are shown in Fig. 4-1. The RE cell temperature was 1300°C and 1100°C for Tb and Er respectively and the RE concentrations were estimated to be about 2 at.% for both samples. The growth procedures were same as that of Eu doped GaN except the RE cell temperatures. Both samples shows clear 1×1 spotty pattern without extra spots suggesting 3D single crystalline growth. The spot pattern from cubic phase of GaN or twins observed in Eu doped GaN were not observed on both sample.

From the X-ray diffraction, only the reflections from GaN (0002) were detected and no secondary phases or cubic GaN were detected. Peak shifts to the lower angle as shown in Fig. 4-2 were observed. No cubic phase introduction was observed in both Tb, Er doped GaN. As the author described in chapter 3, for Eu 2 at.% doped GaN, the strain introduced by the bigger radius of Eu ion was seemed to be rather relaxed by introducing stacking faults. Since the covalent radii of Tb and Er (1.59 and 1.57Å) are in between that of Ga and Eu[4-1], the strain relaxation mechanisms of Tb, Er doped GaN may be different from Eu doped GaN and seem to be rather relaxed by lattice space broadening. Local structures around RE ions were studied by EXAFS analysis. Fig. 4-3 show routine analysis procedure of both Tb (left sides), Er (right sides) doped GaN. The figures on the first low are raw fluorescence intensity data around each absorption edge, the second low are the EXAFS signals χ which are extracted by deduction of background signals and normalization. The third low shows the radial distribution functions (RDF) after Fourier transform. The 4th low shows back Fourier transform of the 1st nearest peaks in RDF, together with that of theoretical parameters calculated by FEFF8 programs. The analytical results thorough curve fitting using theoretical parameters are shown in Table 4-1. Both Tb , Er ions are analyzed to coordinate with nitrogen with coordination number of (roughly) 4 and these mean the incorporations into Ga lattice sites with tetrahedral symmetries.

Table 4-I: Analytical results of Tb, Er- EXAFS measurements

	Eu	Tb
Nearest neighbor atom	Nitrogen	Nitrogen
Coordination Number	3.8	4
Bond length	2.2 Å	2.2Å
Debye-Waller Factor	0.17Å^2	0.06Å^2

Fig. 4-4 shows PL spectra of Tb doped GaN measured at RT (a) and 77K (b). The sample with Tb concentration of 2 at.% shows most strong Tb^{3+} related green emission peak (545nm) while band edgy emission and deep defect level emission of GaN observed as well. Further higher doping of Tb caused concentration quenching which also occurred in Eu doped GaN with Eu concentration higher than 2 at.%. The PL spectra of Er doped GaN with various Er concentrations are shown in Fig.

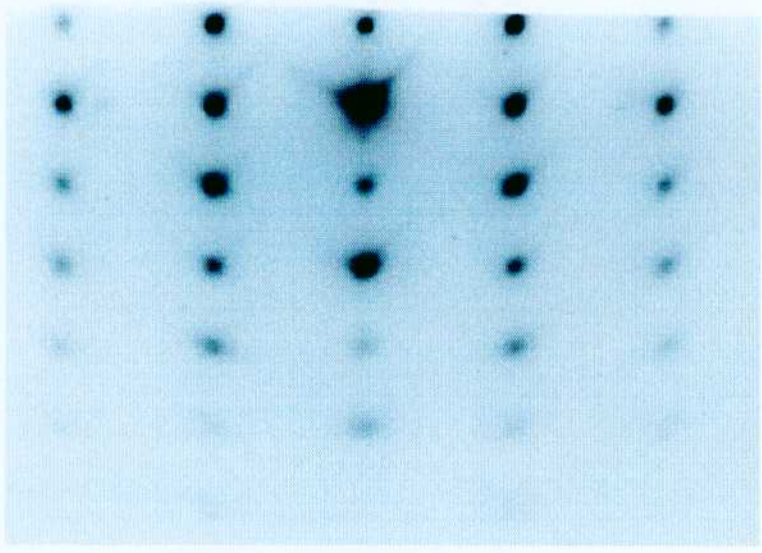

(a)

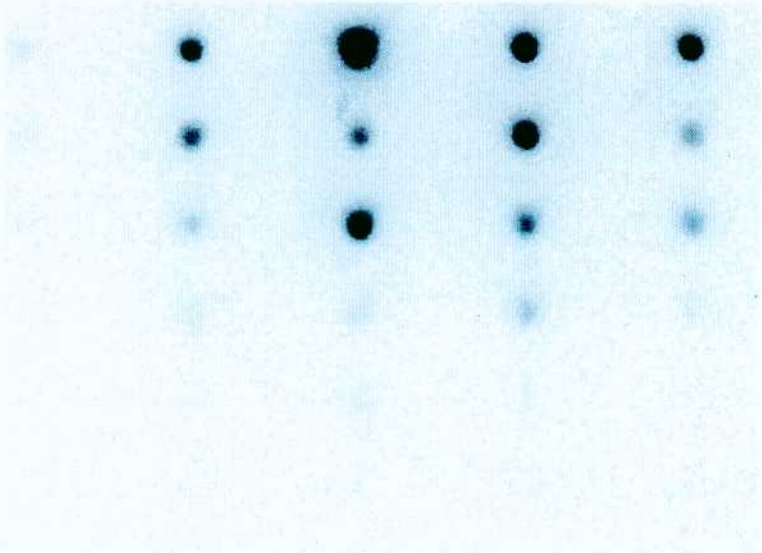

(b)

Figure 4-1: RHEED patterns after 2 hour growth (0.8 m) of (a) Tb:GaN and (b) Er:GaN

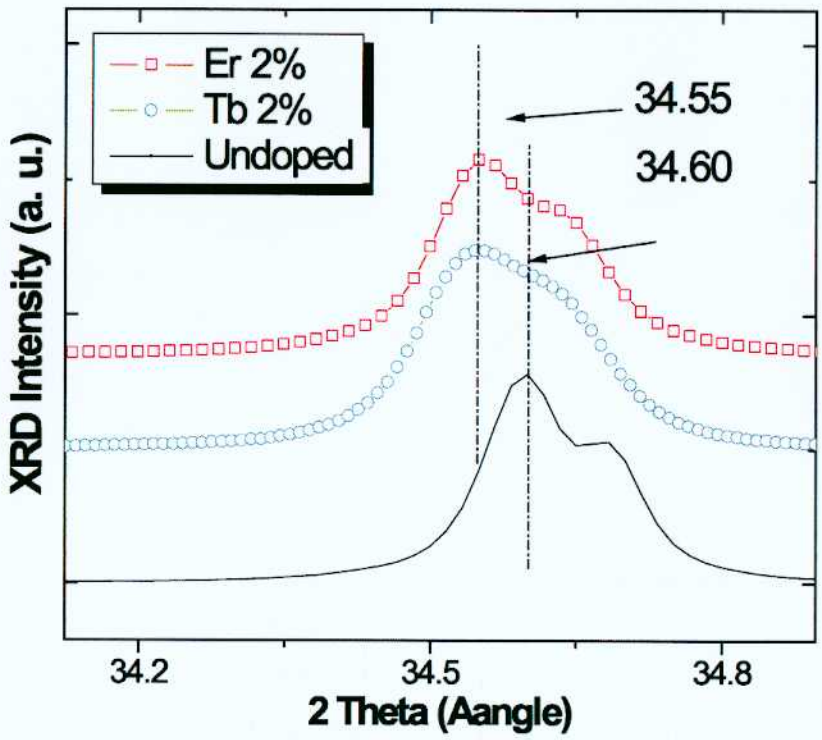

Figure 4-2: XRD profile of Tb doped GaN (o), Er doped GaN (□). Undoped GaN(solid line) are shown as well .

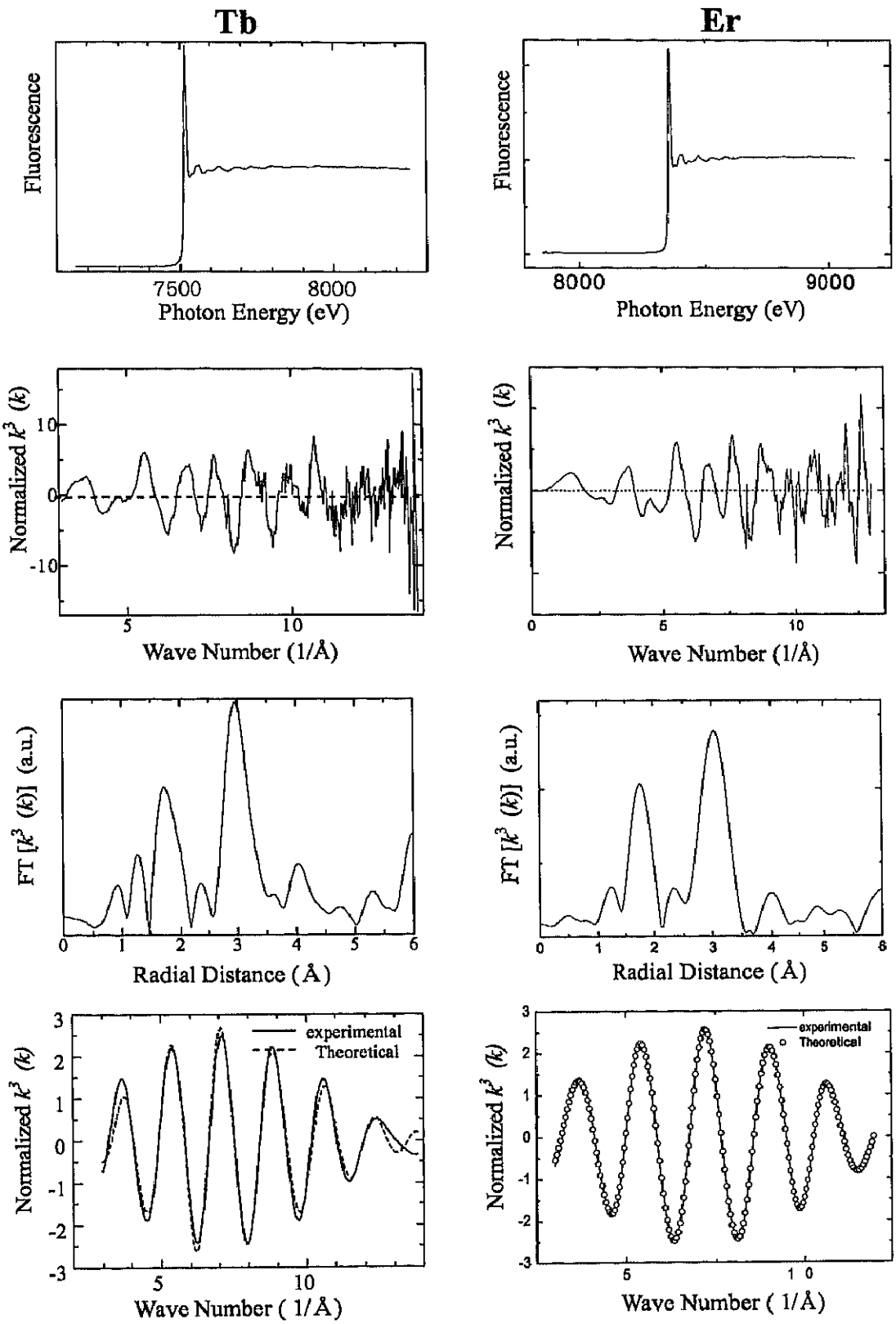

Figure 4-3: Analysis procedure of both Tb (left sides), Er (right sides) doped GaN.

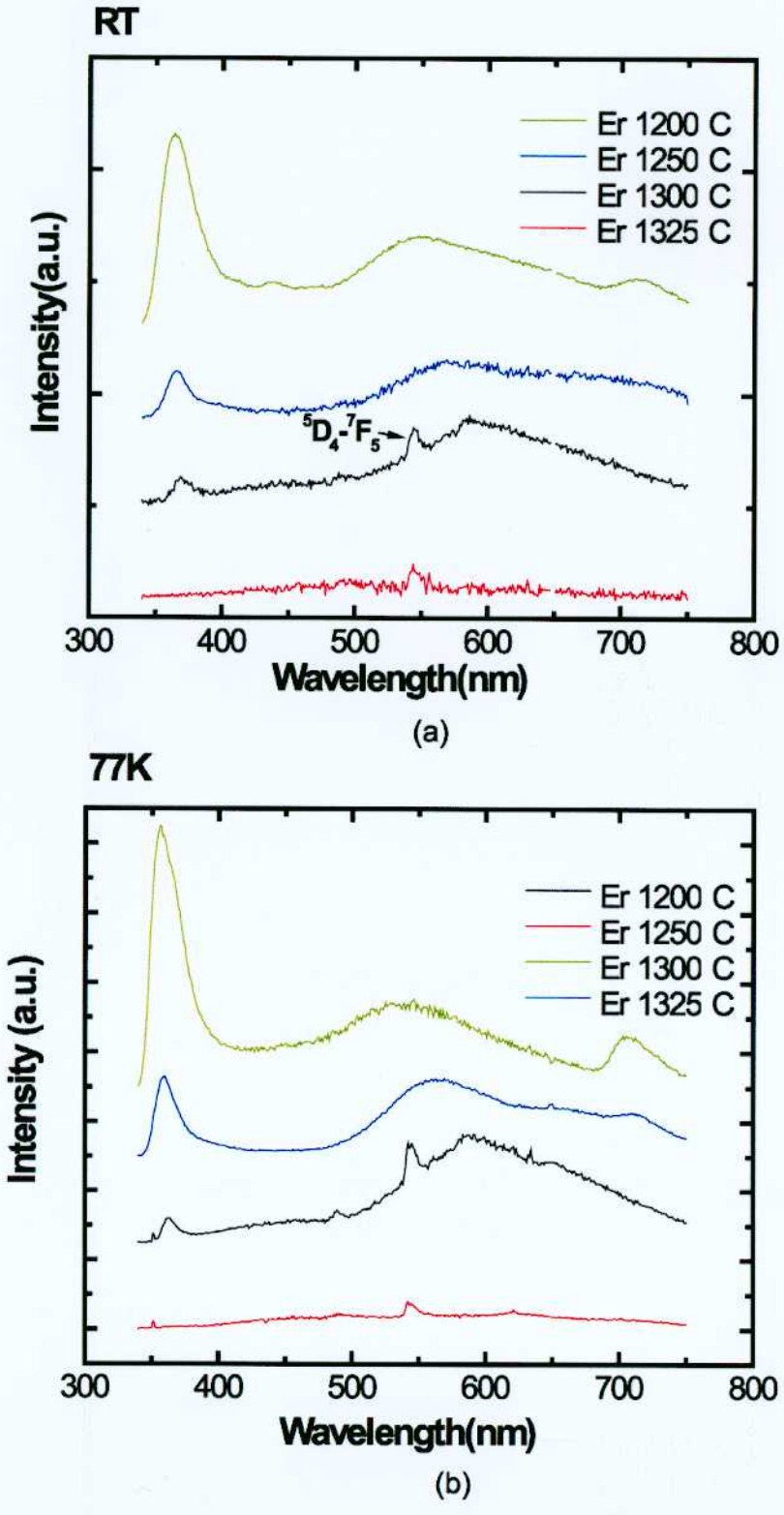

Figure 4-4: PL spectra of Tb doped GaN measured at (a) RT and (b) 77K.

4-5.For the spectra measured at RT, many Er related peaks at green (539, 557nm), and red (670nm) spectral region which are assigned as intra $^3H_{11/2}$-$^4I_{15/2}$, $^4S_{3/2}$-$^4I_{15/2}$, and $^4F_{9/2}$-$^4I_{15/2}$ transitions of Er^{3+} ion[4-2, 3] respectively, were observed. At RT, the red luminescence is rather stronger than green emission while it shows a dominant green emission peak at 557nm at 77K as shown in Fig. 4-5 (a) and (b). The PL spectra of Er-2 at.% doped GaN at RT and 77K are compared in Fig. 4-5 (c). Infra-red emission of $^4I_{13/2}$-$^4I_{15/2}$ transition (1.54μm) at RT is also shown. This wavelength is of interesting region for the application on laser for optical communication using silica fiber.

4.2 Comparative studies with Eu doped GaN.

On Both Tb-doped and Er-doped GaN, emission peaks around green spectral region originating from intra 4f transitions were observed and on Er doped GaN, infra-red emission around 1.54μm was also observed. The intensities of those green emissions, however, are remarkably weaker than that of red emission observed in Eu doped GaN though the concentration of doped RE ions are not so different. The emission intensities are compared in Fig. 4-6. The emission intensity of red emission from Eu^{3+} ion in Eu doped GaN is almost 3 order stronger than green emission of Tb^{3+} ion in Tb doped GaN. To clarify the reason for the remarkable differences in optical properties among RE doped GaN, the author has carried out comparative studies between Eu doped GaN and Tb doped GaN which show stronger and poorer emission intensity respectively.

4.2.1 Difference in Energy transfer efficiency.

Firstly, the author has paid attention to the energy transfer procedures occurring in both Eu, Tb doped GaN. As the author showed in Eu doped GaN, on photoluminescence, Tb ions in Tb doped GaN are also expected to involve mainly on indirect excitation through electron hole pair recombination of GaN host matrix. The author assumed that the efficiency of energy transfer from GaN to Tb ions in Tb doped GaN is much lower than that from GaN to Eu ion in Eu doped GaN. And the low efficiency of energy transfer may result in poorer luminescence intensity. The author suggested a defect-related energy transfer model to explain emission mechanism in Eu doped GaN. Resuming back to the defect related energy transfer model, a defect level was required, in which the recombination of abound excitons would be occurring, and the author has observed a defect level at 0.37eV below the conduction band of GaN in Eu doped GaN. The FTIR absorption spectra of Eu doped GaN and Tb doped GaN together with undoped GaN and sapphire substrate are shown in Fig. 4-7. Except sapphire substrate, the absorption peak around 2950cm^{-1}(0.37eV) was detected in all measured samples including undoped GaN (magnified in the inset of Fig. 4-7) suggesting that the defect-related level is intrinsic property of GaN. Weak but clear absorption peak also observed in Tb doped GaN as well as much stronger absorption peaks were detected in Eu doped GaN. It was also found that the absorption peak intensities are roughly proportional to doping concentration of Eu ion.

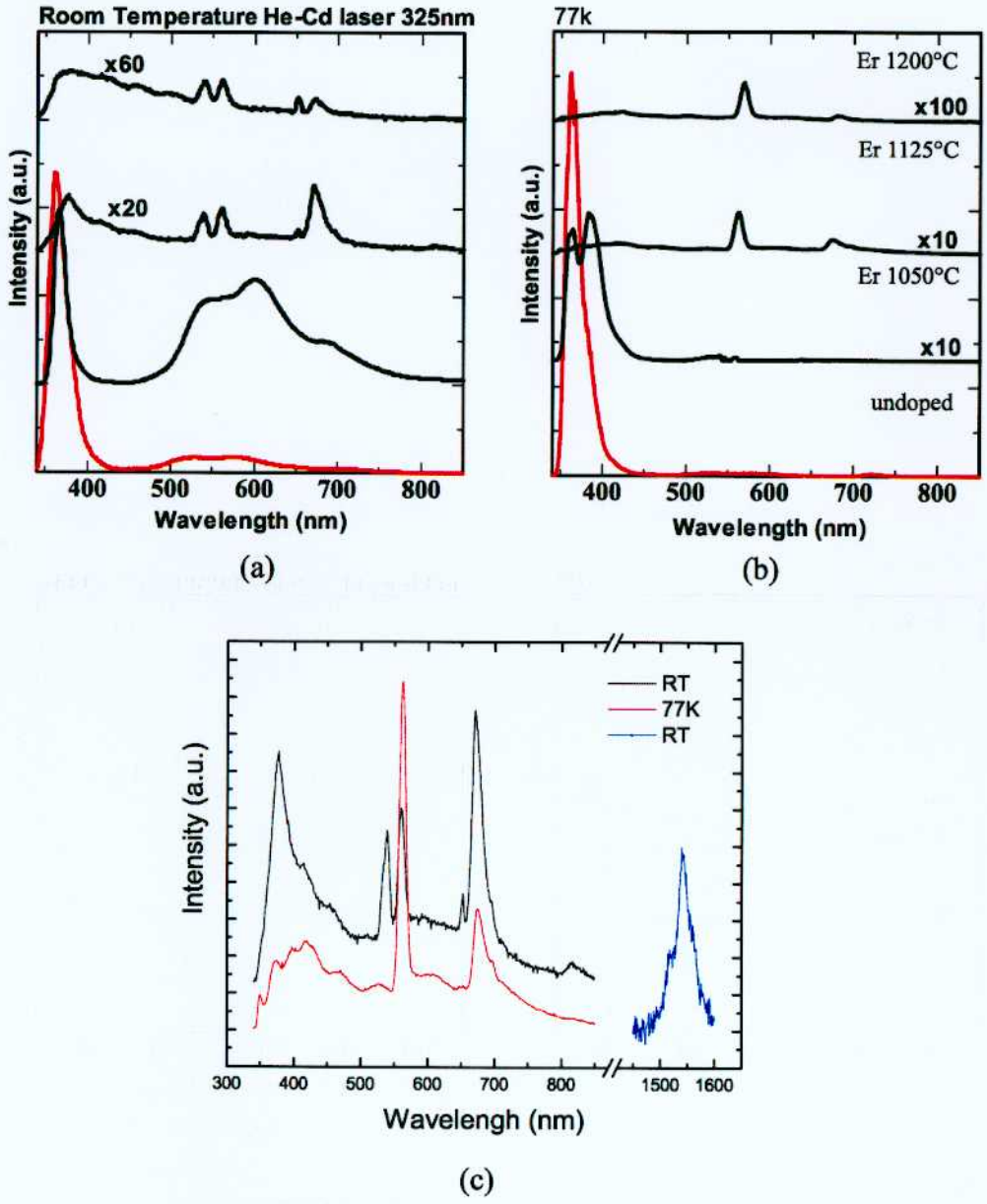

Figure 4-5: PL spectra of Er doped GaN measured at (a) RT and (b) 77K. (c) Green and red infra-red emission from Er 2 at.% doped GaN.

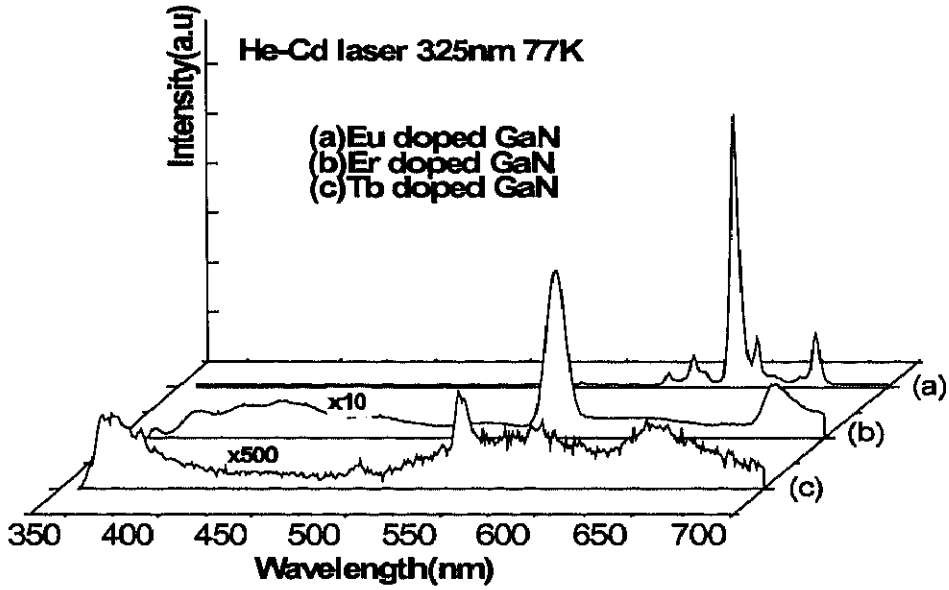

Figure 4-6: PL spectra of (a) Eu doped GaN, (b) Er doped GaN and (c) Tb doped GaN measured at 77K.

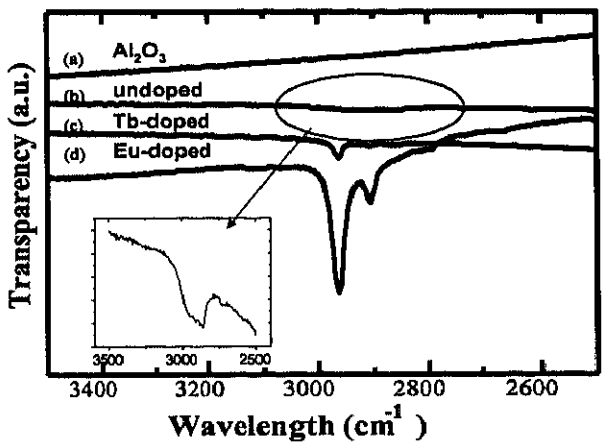

Figure 4-7: FTIR spectra of (a) sapphire substrate, (b) undoped GaN, (c) Tb doped GaN, (d) Eu doped GaN).

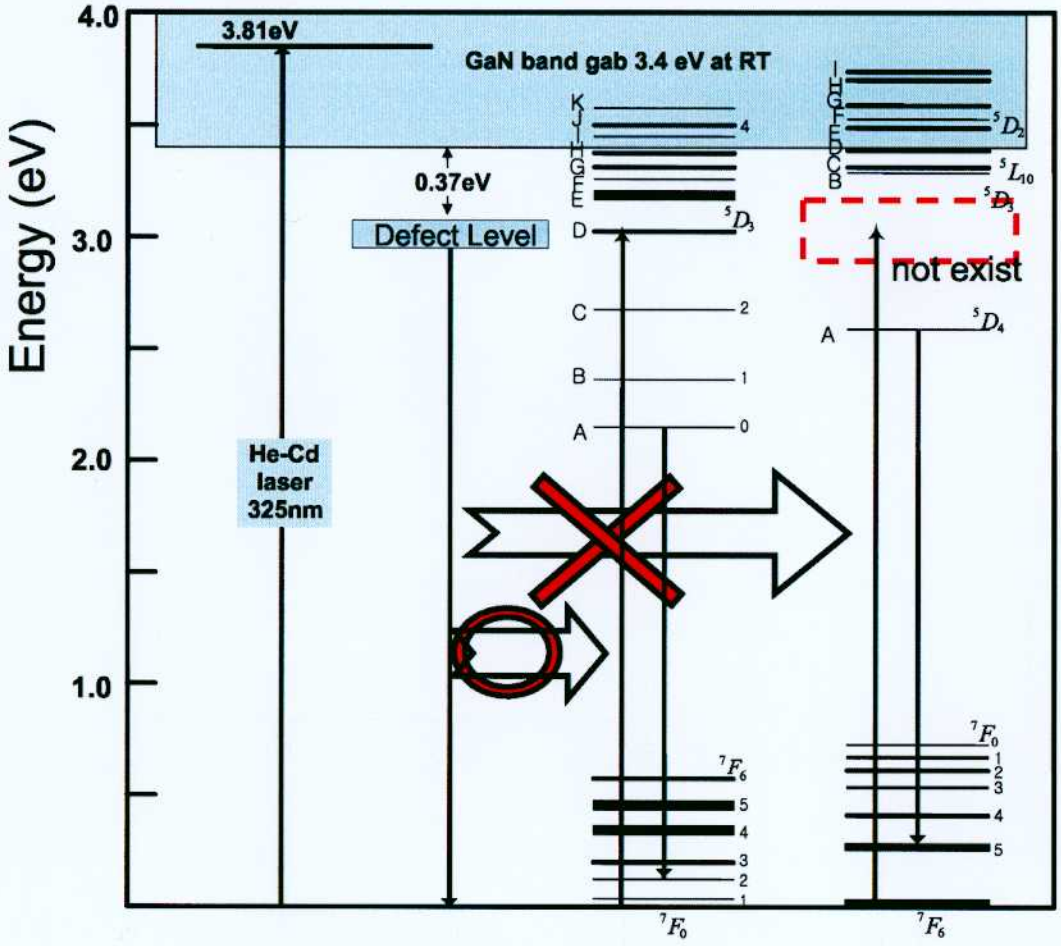

Figure 4-8: Schematic model of energy transfer from GaN to Eu^{3+} or Tb^{3+}.

Now, what does make such a difference in emission intensity? One of the reasons can be considered as follow.

Eu^{3+} ion has an excite energy state ($^5D_3$) from which the energy gap between ground state ($^7F_0$) is almost consistent with the energy gap between observed defect level and top of valance band of GaN (E_{Defect} in Fig. 4-8) as described in Fig. 4-8. This coincidence may heighten the energy transfer efficiency of Eu doped GaN. The defect level in Eu doped GaN is an effective pathway of energy transfer from GaN to Eu ion. On the other hand, there exists no excited state that matches with the defect level in Tb^{3+} as described in Fig. 4-8. Although the energy transfer from GaN host matrix to Tb^{3+} ion can take place through a multi phonon effect, the efficiency is expected to be relatively lower than that of Eu doped GaN. These differences in energy state placing of RE ions related with defect level may be the one of the reason of remarkable differences in emission properties.

4.2.2 Symmetry around RE ions.

From the crystallographical view, the crystal quality of Tb doped GaN does not seem to be inferior to that of Eu doped GaN. As the author has already show in Fig. 3-2, and Fig. 4-1, Tb doped GaN showed RHEED patterns of single crystalline growth while Eu doped GaN showed mixed pattern of cubic and hexagonal phase of GaN although both RE concentrations are almost same (2 at.%). From RBS spectra shown in Fig. 4-9, Eu doped GaN (a) shows inferior crystal quality. Segregation on interface between substrate and GaN film which is not observed in Tb doped GaN (b) was observed. The RBS/C angular distributions of Eu doped GaN and Tb doped GaN are shown in Fig. 4-10. In this experiment also, Tb doped GaN shows superior quality since the depth of dip is more than 80% of the depth of Ga while Eu showed sallow dip depth which is just half of Ga. The satellite peaks observed in Eu doped GaN are not observed in Tb doped GaN. The author supposes a smaller valance radius of Tb than that of Eu is reason for batter crystal quality. The author investigated defect species of Eu doped GaN and Tb doped GaN by monoenergetic positron annihilation method. As shown in Fig. 4-11, the values of S parameter value corresponding to the annihilation of positrons in the Eu: and Tb doped GaN films were larger than the characteristic value of S for the annihilation of positrons from the free-state, or that for positrons trapped by Ga vacancies, suggesting that the major species of defects in the RE:GaN films were vacancy clusters consisting of two or more vacancies. These defects were introduced by replacing Ga with RE elements, and in distortion of the host matrix. The mean open volume of defects in Eu doped GaN was larger than that in Tb doped GaN. This was attributed to the difference between the covalent radii of Eu and Tb.

In GaN film doped with 2at.% Eu, the mean open volume of defects was larger than that in 0.1at.% Eu doped GaN film, but it decreased in 16at.% Eu doped GaN film. In heavily Eu doped GaN film, the decrease in the open volume of defects was associated with the introduction of EuN.

In 2at.% Eu doped GaN film, the mean open volume of defects near the interface between the GaN film and the sapphire substrate was found to be larger than that in the subsurface region. The value of (S, W) corresponding to positron annihilation in the subsurface region lies on the line that connects Tb doped and heavily Eu doped GaN, but the (S, W) value near the interface is located at the right-hand in the subsurface region were different from those near the interface (Fig. 4-12.). The increase in the open volume of defects near the interface could be considered as lowering of coordination symmetry around Eu^{3+} ion. Degradation of crystal quality, which usually decreases emission intensity, is hard to be considered as the reason for the poor emission intensity of Tb doped GaN since all of the above experimental results revealed the superior characters than Eu doped GaN in crystal quality. There may exists another reason for weaker emission intensity of Tb doped GaN.

The symmetry structure around RE ions in inorganic solids is known to be very important factor for emission probabilities (or intensities). Therefore, the author paid attention to the local symmetries around Tb ion and Eu ion. To study local structures around doped RE ions, the author carried out

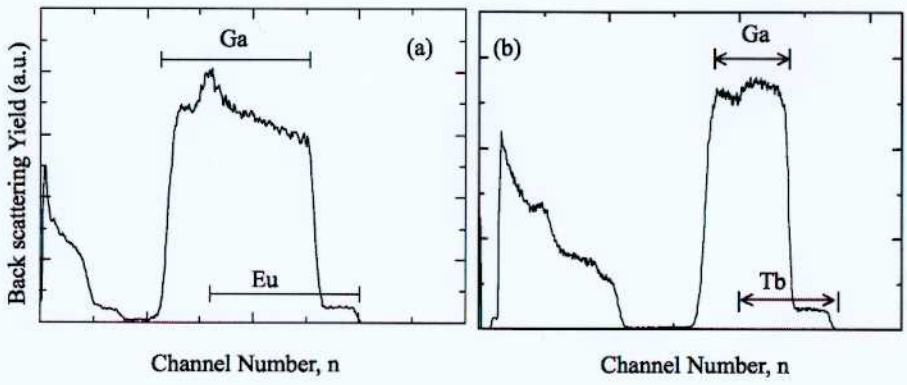

Figure 4-9: RBS spectra of (a) Eu:GaN, and (b) Tb:GaN.

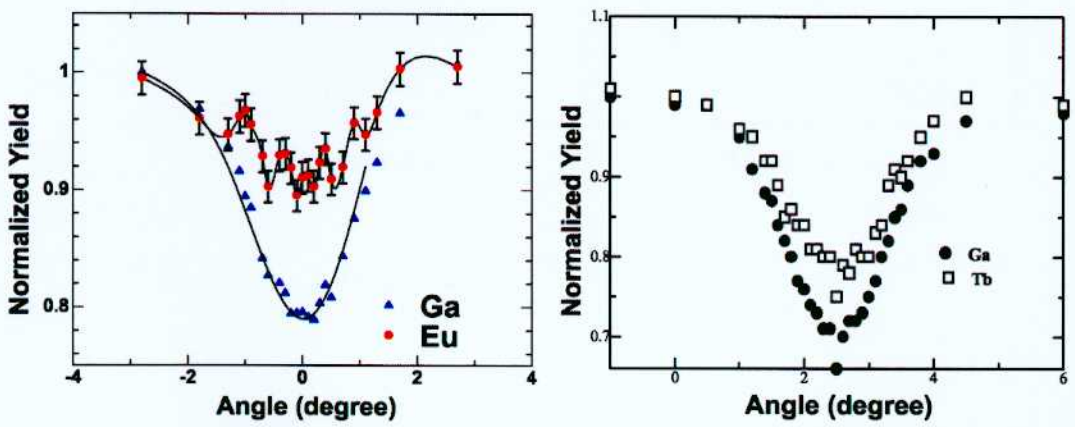

Figure 4-10: RBS/C angular distribution of (a) Eu doped GaN, and (b) Tb doped GaN. The concentrations were both determined to be 2 at.%.

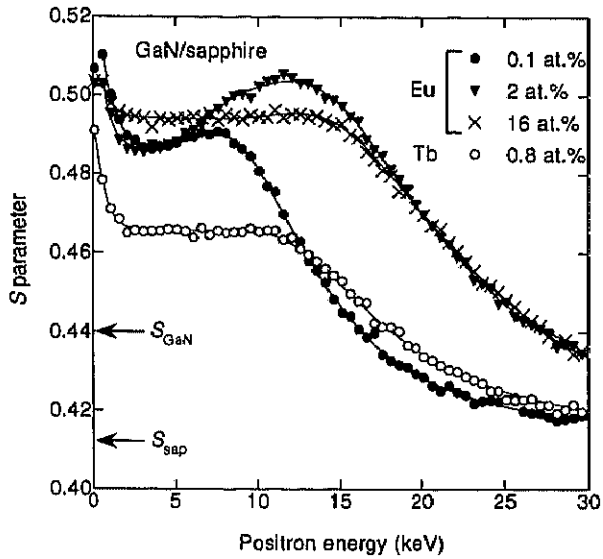

Figure 4-11: S parameter as a function of incident positron energy E for Eu and Tb:GaN/sapphire samples. S for annihilation of positrons in sapphire substrate (S_{sap}) and in high-quality undoped GaN fabricated by MOCVD (S_{GaN}) also shown.

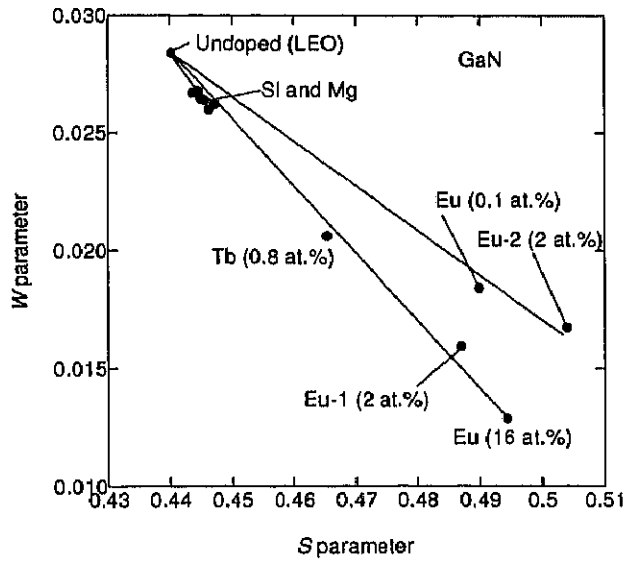

Figure 4-12: S-W plots for Eu and Tb:GaN films. Values of (S,W) for GaN film with Eu concentrations of 0.1 and 16at.% are average values measured at E=6.5~8.5 and 2~11 KeV, respectively. For GaN film doped with 0.2at.% Eu, average value of (S,W) at E=3~5 and 11~13 KeV are indicated by "Eu-1" and "Eu-2", respectively.

EXAFS analysis and the results are shown in Table 4-II. From EXAFS analysis, both Tb and Eu ions analyzed to incorporate into substitutional Ga lattice sites. Tb ions are analyzed to coordinate with 4 surrounding nitrogen in consistent bond length, meanwhile Eu ions turned to have more than one local environment, i.e., 2 kinds of bond lengths with nitrogen were analyzed. The Bonding models are shown in Fig. 4-13. From the results of EXAFS analysis, Eu ions in Eu doped GaN analyzed to have lower coordination symmetry than Tb ions in Tb doped GaN and these are well consistent with the results of above done experiments (RBS, positron annihilation).

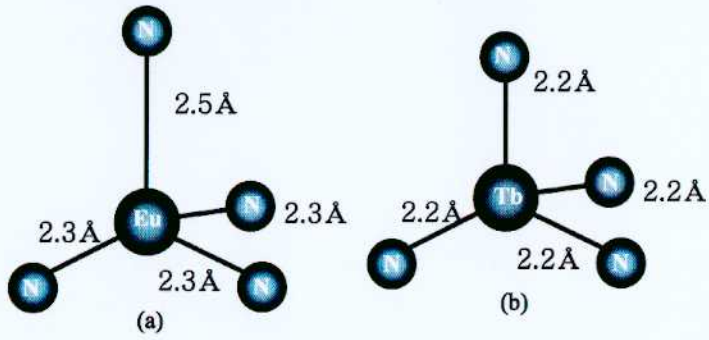

Figure 4-13: Coordination models of (a) Eu:GaN and (b) Tb:GaN

Table 4-II: Analytical results of Eu, Tb- EXAFS measurements

	Eu		Tb
Nearest neighbor atom	Nitrogen		Nitrogen
Coordination number	2.8	0.8	3. 8
Bond length	2.3Å	2.5Å	2.2Å
Debye-Waller Factor	$0.22Å^2$	$0.04Å^2$	$0.17Å^2$

The intra-4f transitions of RE ions, intrinsically, are parity forbidden (only magnetic dipole transition is allowed). But when RE ions are introduced in solids, the electric dipole transitions, which show much bigger transition probabilities than magnetic dipole transition, are partially allowed by crystal field interactions mixing opposite parity wave functions. In the same vein, lowering the coordination symmetry enhances higher transition probabilities[4-4, 5]. The author suggests lower coordination symmetry of Eu ion in Eu doped GaN for cause of stronger emission intensity than Tb doped GaN.

For the summary of this chapter, the author showed green emission from Tb, Er doped GaN, and compared the emission properties with Eu doped GaN. There were remarkable differences on emission intensities between RE:GaN, and the author suggested the mismatching of energy state related with defect level detected in FTIR measurement, and difference in coordination symmetries around RE ion for considerable reasons.

Chapter 4 References

[4-1] http://web.mit.edu/3.091/www/pt/pert5.html

[4-2] G. H. Dieke, Spectra and Energy Levels of Rare Earth Ions in Crystals, pp242, (John Willy & Sons, 1968, New York).

[4-3] M. J. Weber, Phys. Rew. 171, 283 (1968).

[4-4] B. R. Judd, Phys. Rev. 127, 750 (1962).

[4-5] G. S. Ofelt, J. Chem. Phys. 37, 511, (1965).